

COMPUTATIONAL DYNAMICS OF STREAM IN UNDERGROUND STAIRCASE
BY THREE-DIMENSIONAL PARTICLE METHOD

By

Hitoshi Gotoh

Assoc. Prof., Dept. of Urban and Environmental Eng., Kyoto Univ., Kyoto, Japan

Hiroyuki Ikari

Dr. Eng., NEWJEC Inc., Osaka, Japan

Tetsuo Sakai

Prof. Emeritus, Kyoto Univ., Kyoto, Japan

and

Hirokuni Tanioka

Cyubu Regional Development Bureau, Ministry of Land, Infrastructure and Transport, Nagoya, Japan

SYNOPSIS

When a flood occurs, a staircase serves as an escape route from an underground space. Stream in the staircase flows with a high-speed on a steep slope, which is characterized by the appearance of fragmentation of water and splash. To estimate the fluid force acting on a human body during refuge from an underground space, a stream in a staircase must be analyzed. The Lagrangian particle method, which shows good performance to simulate the fragmentation and coalescence of fluid, is applied to a stream in stepped channel. A classification of the flow, which has been shown by previous experiments, is reproduced well by the present 3D particle method. A surface integral of local pressure acting on the model leg is calculated to estimate the hydrodynamic forces on the model leg. The estimated hydrodynamic forces agree well with the results of previous actual-scale hydraulic experiments.

INTRODUCTION

Flood in an urban underground spaces may cause serious damages to people's lives. A refuge from an underground space must be done through a staircase, which is the route of flood intrusion. In the floods, such as those that occurred in Fukuoka in June 1999, and in Tokyo in July 1999, people drowned in the flooding water, which flowed into underground space. Hence it is necessary to study the flow characteristics in a staircase, to save lives. To evaluate a fluid force acting on a human body accurately, a stream on a stair must be analyzed. Toda et al.(15) conducted a hydraulic experiment in the model of staircase of the Hakata-station underground shopping center, with paying attention to inflow discharge. Energy loss of the current and the flow resistance in a stepped channel have been studied (e.g. Yasuda et al., (16); Takahashi et al., (14); Ohtsu et al.(13)). All of these studies are based on physical experiments.

On the other hand, no studies have been based on the numerical simulation, because of the difficulties in computing violent flows. Air pockets, which are formed at the back of a convex corner of steps, and the resultant complicated behavior of water surface in a stepped channel, are difficult to be analyzed by an ordinary Eulerian techniques such as the VOF method. However, the particle method, which has attracted attention as a new free-surface-flow analysis, is suitable for analyzing a rapidly changing flow, because it is the Lagrangian technique treating a definition point of physical properties as a moving particle.

Some aspects of the effectiveness of the particle method had been already demonstrated: a wave breaking on uniform slope by Gotoh and Sakai (3); a wave overtopping on a vertical seawall by Gotoh et al. (6); a flow with drift-timbers by Gotoh et al. (5). Gotoh and Sakai(7) summarized key issues in the application of a particle method to a coastal hydrodynamics. However, all these simulations are two-dimensional ones, although a three-dimensional computation is essential for reproducing actual phenomenon more precisely.

Until recently, 3D computations with sufficient numbers of the particles for realistic conditions have been impossible, due to the limitation of CPU performance. Remarkable progress in developing hardware in recent years has made it possible to carry out the 3D computation in a small domain even by a single CPU. Therefore, in

this study, the MPS (moving particle semi-implicit) method, which is proposed by Koshizuka and Oka(10), was extended to the 3D field. Stream on stepped channel is reproduced by means of the 3D MPS method. To estimate hydrodynamic forces on a human leg in refuge, a drag force is estimated as a surface integral of local pressure acting on the model leg located in a stepped channel.

3D MPS METHOD

The governing equations are the continuity equation and the equation of motion, or the Navier-Stokes equation, as follows:

$$\nabla \cdot (\rho \mathbf{u}) = 0 \quad (1)$$

$$\rho \frac{D\mathbf{u}}{Dt} = -\nabla p + \rho \nu \nabla^2 \mathbf{u} + \rho \mathbf{g} \quad (2)$$

in which, \mathbf{u} =velocity vector, p =pressure, ρ =fluid density, \mathbf{g} =gravitational acceleration vector, and ν = kinematic eddy coefficient.

In the MPS method, calculation points are defined on Lagrangian particles instead of on a computational grid, and the terms in the governing equations are discretized as interactions among particles in the calculated domain. All the terms are calculated with referring to the distance between particles. Therefore, the technique of discretization for the 2D field can be applied to the 3D field, in principle.

The pressure term, or the gradient operator, and the viscous term, or the Laplacian operator, of the i -th particle are written as the interaction among the target particle and other particles existing in the influence sphere of the target particle as follows:

$$-\frac{1}{\rho} [\nabla p]_i = -\frac{1}{\rho} \frac{D_0}{n_0} \sum_{j \neq i} \left[\frac{p_j - p_i}{|r_{ij}|} r_{ij} w(|r_{ij}|) \right] \quad (3)$$

$$\nu [\nabla^2 \mathbf{u}]_i = \frac{2\nu D_0}{n_0 \lambda} \sum_{j \neq i} [(u_j - u_i) w(|r_{ij}|)] \quad (4)$$

$$r_{ij} = r_j - r_i \quad (5)$$

$$w(r) = \begin{cases} \frac{r_c}{r} - 1 & \text{for } r \leq r_c \\ 0 & \text{for } r > r_c \end{cases} \quad (6)$$

in which, D_0 =the number of dimensions, λ =model constant, r_i =position vector of particle, $w(r)$ =weight function, r =distance and r_c =radius of the influence sphere for interaction. All of the above-mentioned equations are similar to the case of two-dimensional calculation(Gotoh et al., (5)).

STREAM IN STAIRCASE

Classification of the Flow Mode

Stream in a staircase, or stream in a stepped channel, is categorized into three regimes: i) skimming flow, which occurs in a steep-slope channel under the comparatively large discharge, ii) nappe flow, which occurs in a mild-slope channel under the comparatively small discharge, and iii) transition flow, which is the transition region of the above two flow regimes (Ohtsu and Yasuda(12)).

Fig. 1 shows a numerical stepped channel, or the calculated domain. One of the sidewalls is not shown in graphics so that the setting of stairs can be easily seen. The soluble moving wall developed by Gotoh et al. (4) is used for the inflow boundary. The moving wall rises in the constant velocity, and the moving-wall particles touching water particles change suddenly into the water particles when their elevation has reached to the threshold value. A constant discharge can be always supplied in a channel. The same numbers of particles are arranged at the lower end of the moving wall, when the moving-wall particles change into the water particles. The outflow boundary, or the end of the stairs, is a free boundary. Hence, the flow depth at the downstream end agrees with the critical depth.

A stepped channel configuration and flow properties are shown in Table 1, in which q =flow discharge per unit width, h =height of stair, l =width of stair in x -direction, and y_c =critical depth ($=(q^2/g)^{1/3}$). Five cases of inflow discharge q are tested for four cases of slope inclinations h/l ; hence the total of 20 cases of calculations are carried out. The number of steps is seven and the diameter of the particle is 1.0 cm. The total number of particles, which depend on the cases, are about 50,000-100,000.

Fig. 2 shows the calculated results plotted together with the experimental flow-regime curves by Yasuda et al.(16) and Chanson(2). In this study, the existence of an air pocket is judged by snapshots of calculated result, and regimes of flow are classified by referring to velocity-vector figures. The agreement of calculated results with the experimental curves is satisfactory.

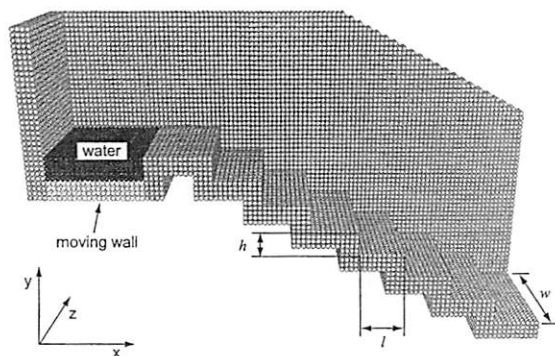


Fig. 1 Numerical stepped channel

Table 1 Calculation condition

	$h/l(\text{cm}/\text{cm})$	$q(\text{m}^2/\text{s})$	h/y_c
Case 1-1	6/15	0.1	0.6
Case 1-2		0.046	1.0
Case 1-3		0.035	1.2
Case 1-4		0.027	1.4
Case 1-5		0.023	1.6
Case 2-1	6/8	0.1	0.6
Case 2-2		0.046	1.0
Case 2-3		0.035	1.2
Case 2-4		0.025	1.5
Case 2-5		0.019	1.8
Case 3-1	6/6	0.064	0.8
Case 3-2		0.046	1.0
Case 3-3		0.031	1.3
Case 3-4		0.019	1.8
Case 3-5		0.015	2.1
Case 4-1	6/5	0.046	1.0
Case 4-2		0.028	1.4
Case 4-3		0.019	1.8
Case 4-4		0.014	2.2
Case 4-5		0.012	2.5

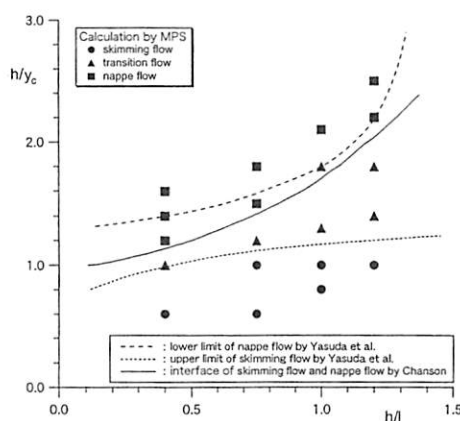


Fig. 2 Flow regime classification

Calculated results of a skimming flow (Case1-1) are shown in Figs. 3 and 4. Fig. 3 shows a snapshot at $t=9.3\text{s}$, in which the particles are shown in the gray-scale to identify the level of their velocity. Air pocket cannot be seen in a concave corner. Moreover, the velocity in the concave corner of the steps is almost less than 10% of the mainstream velocity, in other words, a dead water region is formed at a concave corner. Because the pressure change of a gas phase in the air pocket cannot be treated in a single-phase flow model, it cannot be said strictly that an air pocket is reproduced, however, a closed region, in which water particles do not exist, is defined as an air pocket. Fig. 4 shows the instantaneous velocity distribution at Eulerian observation points, which is located uniformly with 1.0 cm spacing in x - and y -directions. Time-averaged velocity for five seconds after the flow becomes steady is plotted. Remarkable circulating flow can be seen in a concave corner of steps, and the mainstream flows in almost a parallel direction to a pseudo-bottom that is defined by the line linking convex edges of steps. These characteristics show the same tendency as sketched by Ohtsu et al.(13).

In Figs. 5 and 6, calculated results of a nappe flow (Case1-5) are shown. The velocity vector of mainstream does not have a uni-directionality, which is seen in velocity vector diagram of a skimming flow. In the mainstream, a dropping jet flows down with repeating collision and repulsion with upper faces of steps. Air pockets are formed at the front of a vertical wall of steps. Air pockets exist stably through a total computation process. In the concave corner of the steps, a dead water region is formed just like a skimming flow. These characteristics of the calculated results show a similar tendency with the results of observations in the experiment by Ohtsu et al.(13). In the case of nappe flow, an appearance frequency of splash is high, because the mainstream hits upper faces of steps.

Velocity Profile

A velocity profile of a skimming flow in the normal direction of a pseudo bottom at the center of a channel was

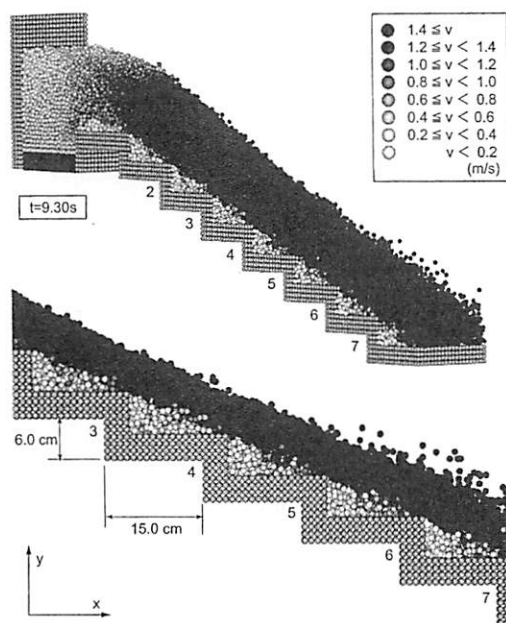


Fig. 3 Snapshot (skimming flow)

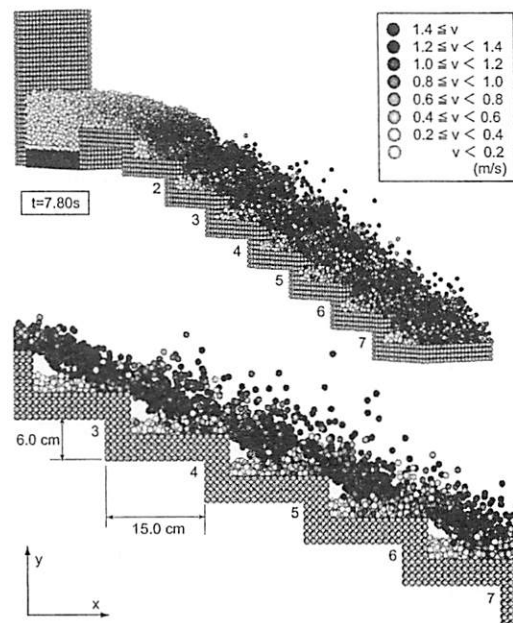


Fig. 5 Snapshot (nappe flow)

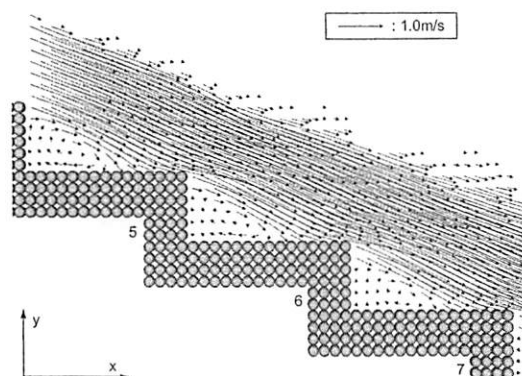


Fig. 4 Velocity vector (skimming flow)

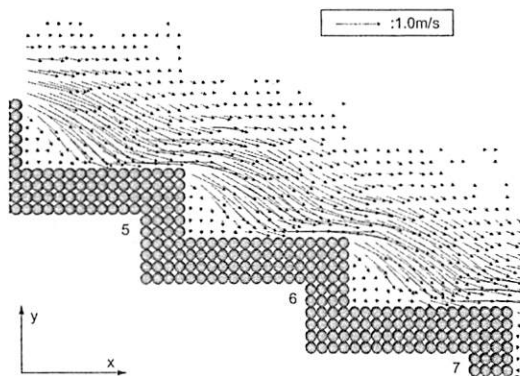


Fig. 6 Velocity vector (nappe flow)

measured by Bose and Hager(1). In the calculation, the same flow discharge as the experiment by Bose and Hager is given to satisfy the relation $y_c/h=1.2$ under the slope inclination $h/l=5/3$. All the configurations of the calculated domain are the same as the experimental flume of Bose and Hager.

The channel width is 0.5 m. Total particle number is about 200,000 under a steady state. An instantaneous snapshot at $t=16.0$ s is shown in Fig. 7. The Eulerian observation points are arranged in 5mm spacing in the normal direction of a pseudo bottom. The origin of the measuring points is set to the edge of the twelfth step from the top.

The velocity profile is shown in Fig. 8. Without a scaling, or a non-dimensionalization, a calculated flow velocity shows a satisfactory agreement with the experimental results. But, in detail, in the wall neighboring part, a calculated velocity gradient is higher than that of the experimental results. At $y=0.015$ m, a change of a calculated velocity gradient is clearly found, while the experimental results show a more gradual transition of velocity gradient.

HYDRODYNAMIC FORCE ON A HUMAN-LEG IN FLOODING STAIRCASE

Estimation of Hydrodynamic Force on a Human-Leg Model

Fig. 9 shows the computational leg model made of particles, the rough shape which agrees with the human-

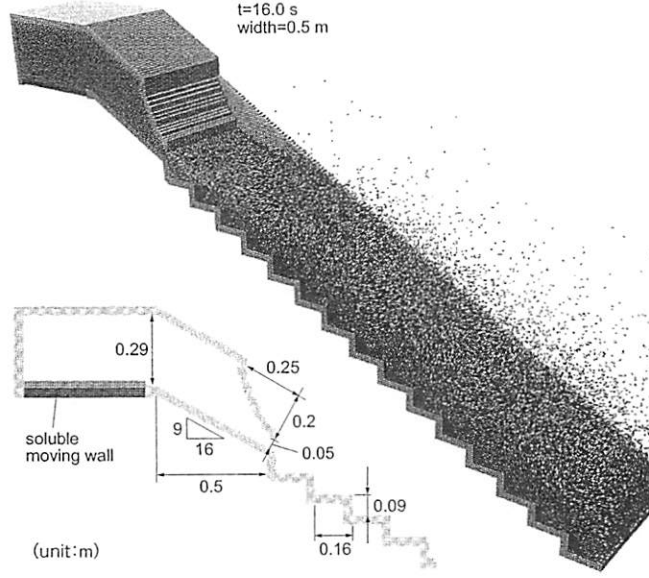


Fig. 7 Snapshot and control surface

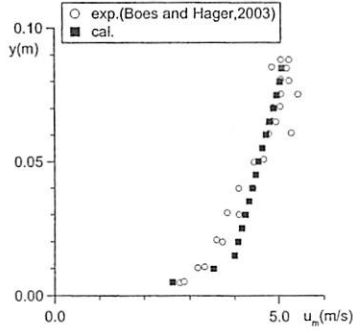


Fig. 8 Velocity profile

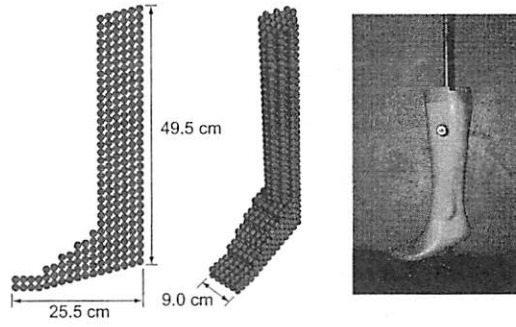


Fig. 9 Computational leg model and photo of leg model for experiment by Ishigaki et al.

leg model in the hydraulic experiment by Ishigaki et al.(9). They attached the human-leg model on one side of the balance the fulcrum of which is located 50.0 cm above from the surface of the steps as a model of a knee. On the other side of the balance, a load cell is set on a support at the end to measure the hydrodynamic forces.

In this study, a hydrodynamic force is estimated in the following way. By supposing a pressure to be a fluid stress on the surface of the leg model, the force acting on the leg model can be written as follows:

$$F = - \int_S p n dA \quad (7)$$

in which, S =surface of the leg model in the underwater, n =unit vector in the normal direction of a leg surface, the positive sign of which goes outward of the leg model, and dA =area element of a leg surface. By defining the unit vector in the streamwise direction (x direction) as ξ_x , the streamwise component of the hydrodynamic force F_x can be written as follows:

$$F_x = F \cdot \xi_x = - \int_S p n \cdot \xi_x dA = - \int_S p n_x dA \quad (8)$$

in which, n_x =streamwise component of a unit vector in the normal direction of a leg surface n . By assuming the square, the one side of which is d_i (particle size) as an area element, Eq. 8 can be discretized as

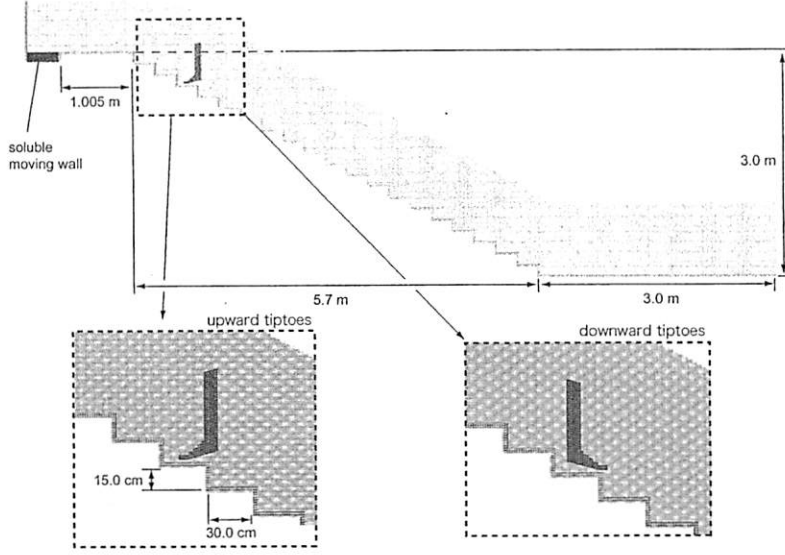


Fig. 10 Staircase model (Calculated domain)

$$F_z = \sum_{i=1}^{N_{leg}} p_i n_{zi} d_i^2 \quad (9)$$

in which, N_{leg} =the number of constituent particle of the leg surface.

To determine the normal direction of a leg surface on the particle i , the method of estimating the normal direction of water surface applied in the surface tension model of the 2D MPS method(see Nomura et al.(11)) is extended to the 3D field. In other words, the unit vector in the normal direction is written as:

$$a_i = \frac{n_i^{+x} - n_i^{-x}}{2l_0} n_x + \frac{n_i^{+y} - n_i^{-y}}{2l_0} n_y + \frac{n_i^{+z} - n_i^{-z}}{2l_0} n_z \quad (10)$$

$$n_i = \frac{a_i}{|a_i|} = (n_{xi}, n_{yi}, n_{zi}) \quad (11)$$

in which, l_0 =spacing between particles, and $n_i^{\pm x}(r_i \pm l_0 n_x)$, $n_i^{\pm y}(r_i \pm l_0 n_y)$, $n_i^{\pm z}(r_i \pm l_0 n_z)$ =the particle number density of six points around the particle i . For computing the particle number density herein, a tophat-shape weight function is applied as follows:

$$w_f(r) = \begin{cases} 1 & \text{for } r \leq r_e \\ 0 & \text{for } r > r_e \end{cases} \quad (12)$$

In addition, only the contributions of the leg constituent particles are counted in this calculation. The diameter of the weight function is set at $r_e = 3.1 d_i$.

Comparison with Hydraulic Experiment

Fig. 10 shows the staircase model, or the calculated domain, whose specifications are similar to the experiment performed by Ishigaki et al.(9). In the staircase section, steps the top-surface of which is 30.0 cm long and 100.5 cm wide, are set. The total number of steps is 20 and the height of steps is 15.0 cm. The leg model is installed at the center on the 17th step from the bottom of staircase. A constant discharge is supplied by the soluble moving wall(4) at the left end of the channel. The inflow discharge per unit width is given to set the ground water depth $h_{gt} = 0.2, 0.3$ and 0.4 m, according to the experimental formula:

$$q = 1.98 h_{gt}^{1.62} \quad (13)$$

proposed by Ishigaki et al.(9). For each setting of inflow discharge, Ishigaki et al. carried out experiments for the two directions of a tiptoe, upstairs-ward and downstairs-ward. The downstream end of calculated domain is free outflow boundary, hence, at the outflow boundary, a depth of water is equal to the critical depth. The diameter of particle is 1.5 cm. The total numbers of particles for the ground water depths $h_{gt} = 0.2, 0.3$ and 0.4 m are approximately 700,000, 800,000 and 1,000,000, respectively.

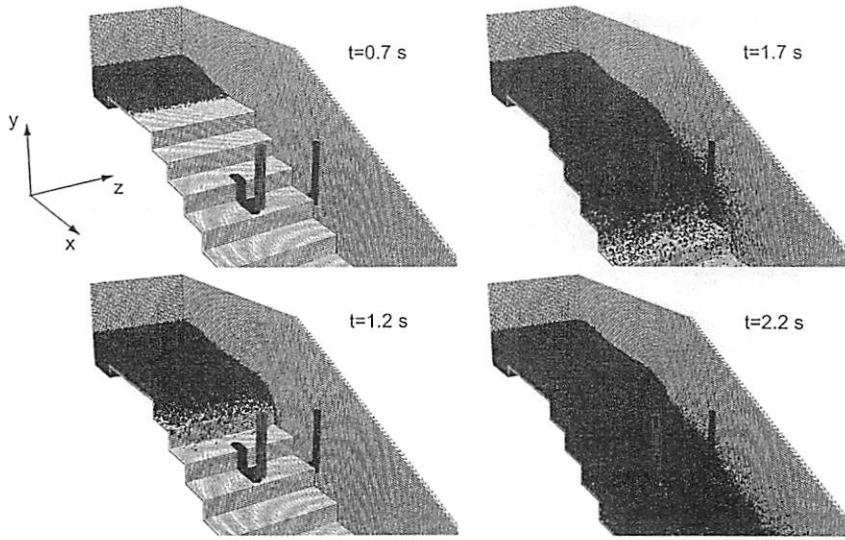


Fig. 11 Snapshots of flow in staircase

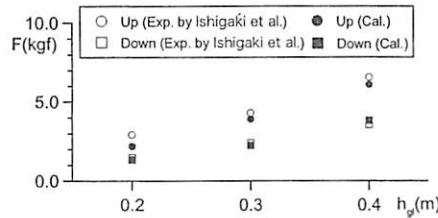


Fig. 12 Calculated hydraulic forces on leg model in staircase

Some snapshots of calculated results are shown in Fig. 11. Stream collides with the leg model and flows down causing a splash. The averaged value of the time averaged velocities at the observation points in a water surface at the center of seven steps, which are from the 7th step to the 13th step from the bottom of staircase, are 2.3, 3.7 and 4.4 m/s for the ground water depths $h_{gt}=0.2, 0.3$ and 0.4 m, respectively. Ishigaki et al. estimated the velocity averaged over water-surface from video images of colored ball as a tracer. The measured velocity averaged over water-surface are 2.8, 4.0 and 4.8 m/s for the ground water depths $h_{gt}=0.2, 0.3$ and 0.4 m, respectively. Fig. 12 shows the calculated hydraulic forces together with the experimental results reported by Ishigaki et al.(9). In the hydraulic experiment, a hydraulic force is estimated for the leg model with wearing sneaker by assuming that a load concentrates on the height of an ankle. It is suggested that a form drag is more predominant than a frictional resistance, which depends on whether the sneaker is worn or not, because the hydraulic force calculated without considering a skin friction agrees well with an experimental result.

Flow around Leg Model in Staircase

In order to consider the difference in hydrodynamic forces of two directions of a tiptoe, upstairs-ward and downstairs-ward, flow field is examined. Water depth distribution around a leg model in the case of $h_{gt}=0.4$ m is shown in Fig. 13. The water depth h is defined as the distance between a pseudo-bottom and a water surface. The elevation of a water surface is estimated as the highest position of particles among which free surface particles of the MPS method satisfying the condition $n_i < \beta n_0$ are excluded. Both regimes of the flow field in two directions of a tiptoe are supercritical: the Froude numbers, in which the water depth and the velocity are calculated as the averaged values in the region shown by the dashed rectangle in Fig. 13, are 2.7 and 2.2 for the upstairs-ward and downstairs-ward tiptoes, respectively.

Fluctuation of a water surface propagates only to the downstream direction of the leg model, and a low water-depth domain appears in the wake region of the leg model. The Mach angle β_0 , which is defined as the angle between two fronts of shock waves shown in a dashed lines in Fig. 13, are 23.4 and 27.3 for the upstairs-ward and downstairs-ward tiptoes, respectively. It goes without saying that the linear shock wave front, that can be observed in a high

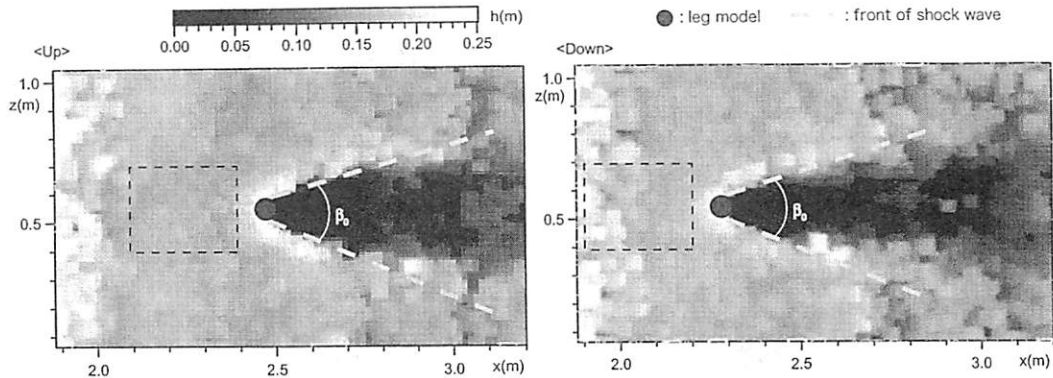


Fig. 13 Water depth distribution around a leg model

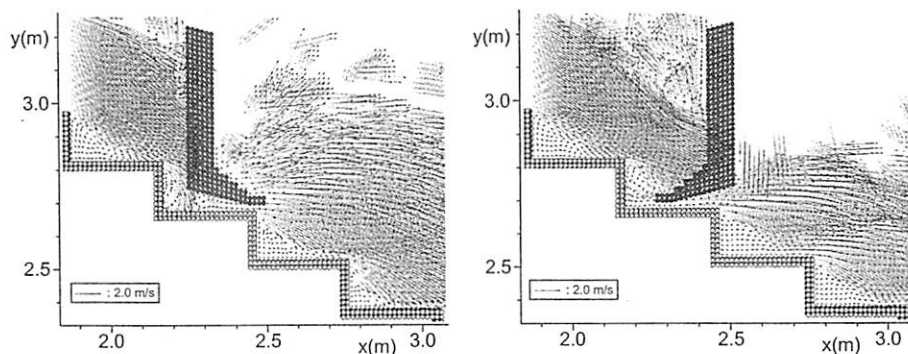


Fig. 14 Velocity vector in the central cross section

speed flow on a flat bottom, is not found in this calculation, because a bottom is stepped, and the unsteadiness of water-surface profile in the wake region is intense. The Mach angle β_0 is defined as:

$$\beta_0 = \sin^{-1}(V_{us} / \sqrt{gh_{us}}) \quad (14)$$

in which, h_{us} =averaged water depth and V_{us} =averaged mainstreamwise component of velocity in the upstream region with streamwise and transverse widths 0.3 m (shown by the dashed rectangle in Fig. 13) are 21.4 and 27.1 for the upstairs-ward and downstairs-ward tiptoes. These values agree well with the values calculated by the angle between two fronts of shock waves.

Fig. 14 shows the velocity vector distribution in the central cross section of a channel. Where the time averaged values during 0.5 s around the time $t=3.5$ s, at the Eulerian observation points spaced by 1.0 cm in x and y directions are displayed. In both figures, a separating vortex at the concave corner of the steps, which characterizes a skimming flow, are found on the upstreamside step of the leg model. In addition, clear vortex structures can be observed between an instep and a perpendicular face of a step for the upstairs-ward tiptoe, between a heel and perpendicular face of a step for the downstairs-ward tiptoe, respectively. However, the reason for the difference in hydrodynamic forces acting on the upstairs-ward and downstairs-ward tiptoes is not clear based on the characteristics of flow field in a vertical 2D plane.

Fig. 15 shows the velocity vector distribution in the horizontal cross section, or a x - z plane, at the elevation $y=2.745$ m crossing a heel. Velocities at the Eulerian observation points spaced by 1.0 cm in x and z directions are displayed. The flow colliding with an instep of leg turns to the z axis direction. A large-scale outward flow due to the turn of a main stream makes the separating streamline moving to the outside, or the far side of leg, consequently, a wake region is enlarged. On the other hand, although the flow colliding with a heel of leg turns to go along a surface of a heel, the scale of the outward flow due to this turn of a main stream is smaller than that of flow field around a the upstairs-ward tiptoe. Consequently, the wake region of leg is smaller than of the upstairs-ward tiptoe. This difference of a streamline is due to the difference of the configuration of horizontal cross section of leg model in upstairs-ward and downstairs-ward tiptoes. It is known that a drag coefficient of a square pillar, one side of which is normal to the streamwise direction, is as twice larger as the drag coefficient of a column, whose diameter is the same as one side of

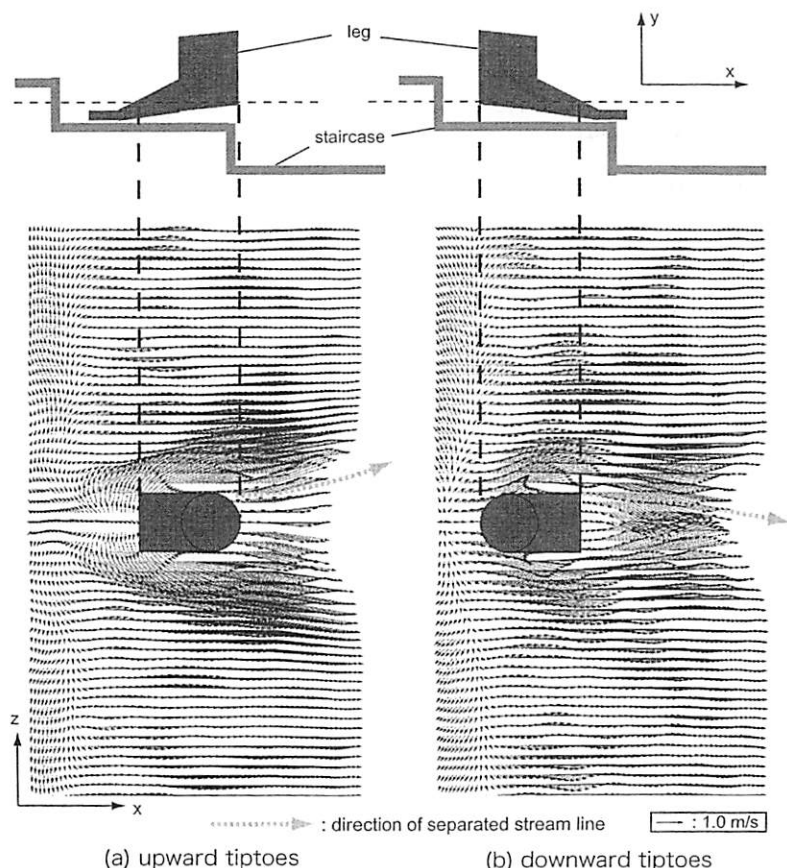


Fig. 15 velocity vector in the horizontal cross section

a square pillar(8). This fact supports some of the difference of hydrodynamic forces of upstairs-ward and downstairs-ward tiptoes.

CONCLUSIONS

In this study, stream in a staircase and a resultant hydrodynamic forces acting on a human leg were analyzed by the Lagrangian particle method, as fundamental information of refuge from an underground space in a flood.

The flow regime in a stepped channel, such as a skimming flow and a nappe flow, which was previously found in hydraulic experiments, was reproduced well by the particle method. The calculated velocity profile showed satisfactory agreement with the previous experimental result.

Hydrodynamic forces acting on the human leg on stepped channel were calculated by the particle method. The experimental result reported by Ishigaki et al. was reproduced well by means of the particle method. The difference of hydrodynamic force on directions of the tiptoe, upstairs-ward and downstairs-ward, which was found in the experiment, was explained with investigating the flow-velocity field around a leg model numerically.

A geometrical configuration of the staircase and the position of the human body in a staircase, center or wall neighborhood, should be one of the key issues to be investigated in a future from a viewpoint of computational science.

ACKNOWLEDGEMENT

Authors wish to express our gratitude to Prof. Taisuke Ishigaki, Kansai University, for providing us valuable experimental data and useful advice in planning of computation. Authors also wish to express our gratitude to Prof. Keiichi Toda, Disaster Prevention Research Institute, Kyoto University, for precious comments of characteristics of flood in urban underground space.

REFERENCES

1. Bose, R. and W.H. Hager: Two-phase flow characteristics of stepped spillways, *Journal of Hydraulic Engineering*, ASCE, Vol. 129, No.9, pp. 661-670, 2003.
2. Chanson, H.: *Hydraulic design of stepped cascades, channels, weirs, and spillways*, Pergamon, Oxford, UK, 1995.
3. Gotoh, H. and T. Sakai: Lagrangian simulation of breaking waves using particle method, *Coastal Eng. Jour.*, Vol. 41, Nos. 3 and 4, pp.303-326, 1999.
4. Gotoh, H., Shibahara, T. and T. Sakai: Sub-particle-scale turbulence model for the MPS method -Lagrangian flow model for hydraulic engineering-, *Computational Fluid Dynamics Journal*, Vol. 9-4, pp. 339-347, 2001.
5. Gotoh, H., Sakai, T. and M. Hayashi: Lagrangian model of drift-timbers induced flood by using Moving Particle Semi-Implicit method, *Jour. Hydroscience and Hydraulic Engrg.*, JSCE, Vol.20, No.1, pp. 95-102, 2002.
6. Gotoh, H., Ikari, H., Memita, T. and T. Sakai: Lagrangian particle method for simulation of wave overtopping on a vertical seawall, *Coastal Eng. Jour.*, Vol. 47, Nos. 2-3, pp.157-181, 2005.
7. Gotoh, H. and T. Sakai: Key issues in the particle method for computation of wave breaking, *Coastal Eng.*, Vol. 53, No. 2-3, pp.171-179, 2006.
8. Igarashi, T.: Characteristics of the flow around rectangular cylinders (The case of the angle of attack 0 deg), *Trans. of JSME, Series B*, Vol. 50, No. 84, pp. 3185-3192, 1984 (in Japanese).
9. Ishigaki, T., Baba, Y., Toda, K. and K. Inoue: Experimental study on evacuation from underground space in urban flood, *Proc. of XXXI IAHR Congress*, Seoul, 2005. (on CD-ROM)
10. Koshizuka, S. and Y. Oka: Moving-particle semi-implicit method for fragmentation of incompressible fluid, *Nuclear Science and Engineering*, Vol. 123, pp. 421-434, 1996.
11. Nomura, K., Koshizuka, S., Oka, Y. and H. Obata: Numerical analysis of droplet breakup behavior using particle method, *Jour. Nucl. Sci. and Tech.*, Vol. 38, No.12, pp.1057-1064, 2001.
12. Ohtsu, I. and Y. Yasuda: Characteristics of flow condition on stepped channels, *The 27th Cong. of IAHR, Water Resources Engineering*, Div./ASCE. San Francisco, USA, pp. 538-588, 1997.
13. Ohtsu, I., Yasuda, Y. and M. Takahashi: Flow characteristics of skimming flows in Stepped Channels, *Jour. Hydraulic Eng.*, Vol. 130, No.9, ASCE, pp. 860-869, 2004.
14. Takahashi, M., Yasuda, Y. and I. Ohtsu: Energy loss of supercritical flows in stepped channel flows, *Annual Journal of Hydraulic Engineering*, Vol. 48, pp. 871-876, 2004(in Japanese).
15. Toda, A., Inoue, T., Honda, Y. and K. Furumoto: Experimental study on the evaluation on discharge of inundating water flowed over straight stair to underground space, *Annual Journal of Hydraulic Engineering*, Vol. 45, pp. 901-906, 2001 (in Japanese).
16. Yasuda, Y., Takahashi, M. and I. Ohtsu: Flow resistance of stepped channel flows, *Annual Journal of Hydraulic Engineering*, Vol. 44, pp. 527-532, 2000 (in Japanese).

(Received September 1, 2006 ; revised January 9, 2007)